

Investigation of liquefaction-induced lateral load on pile group behind quay wall



Chunhui Liu^a, Liang Tang^{a,*}, Xianzhang Ling^a, Lijun Deng^b, Lei Su^a, Xiaoyu Zhang^a

^a School of Civil Engineering, Harbin Institute of Technology, Harbin, Heilongjiang 150090, China

^b Department of Civil and Environmental Engineering, University of Alberta, Edmonton, Alberta, Canada T6G1H9

ARTICLE INFO

Keywords:

Pile group
Liquefaction-induced lateral spreading
Liquefied soil pressure
Shake-table test
Finite element analysis

ABSTRACT

This paper presents the results of a shake-table test on a 2×2 pile group behind a quay wall. The main objective is to study the behavior of the pile group under the liquefaction-induced lateral spreading and the liquefied soil pressure exerted on the individual pile in the pile group. The test results are presented and discussed. Significant pile group effect is observed through a comparison of the monotonic bending moments of the individual pile in the pile group. In this regard, a simple finite element model is developed to evaluate the liquefied soil pressure on the individual pile in the pile group, in which, both the uniform and triangular soil pressures are calibrated based on the tested monotonic bending moments of the piles. The liquefied soil pressure on the pile near the quay wall is about twice as much as that on the pile far from the quay wall. Next, the liquefied soil pressure on the individual pile in the pile group is compared to that obtained from the shake-table test on single pile. Further, a parametric study is conducted to investigate the effect of the pile rotational stiffness and the pile diameter on the pile group response. Finally, the concluding remarks are drawn based upon the presented results.

1. Introduction

Numerous case histories of the pile foundation damage or failure caused by liquefaction-induced lateral spreading have been reported in major earthquakes, such as 1964 Niigata earthquake [1], 1989 Loma Prieta earthquake [2], 1995 Kobe earthquake [3], 1999 Chi-Chi earthquake [4], 2001 Arequipa earthquake [5], and 2011 Christchurch earthquake [6]. Documentation and analysis of these case histories have highlighted the importance of the kinematic soil-pile interaction, i.e., the lateral load on the pile foundations caused by the lateral spreading of liquefied soil [7,8]. Therefore, a proper consideration of the kinematic effect is one of the most important aspect of pile design, however, this effect has not been fully understood in current study, which is either ignored or crudely approximated in the pile design code.

To investigate the soil-pile kinematic interaction, the pile behind water front structures was studied using laboratory tests and field investigations. With the results of centrifuge tests on a 2×3 pile group behind a wall in the lateral spreading ground, Sato [9] suggested that piles near the quay wall suffered more severe damage than those far from the quay wall. Sato and Tabata [10] studied soil liquefaction and the lateral spreading of saturated sand behind a sheet-pile wall using a large-scale shake-table test, and they found that the excess pore water pressure increased after a few cycles of shaking, and the loss of effective

stress could further lead to the lateral spreading of liquefied sand. Motamed et al. [11] conducted shake-table tests on a 3×3 pile group behind a sheet-pile quay wall, and they concluded that the lateral soil pressure on the pile foundations induced by the lateral spreading was dependent upon the position of the individual pile in the group. Motamed et al. [12,13] performed large-scale shake-table tests on a 2×3 pile group behind a sheet-pile quay wall, the test results indicated that the piles close to the quay wall experienced larger lateral forces than the piles far from the quay wall. Ashford et al. [14] conducted a full-scale field test in which the controlled blasting was adopted to induce liquefaction and liquefaction-induced lateral spreading, and assessed the behavior of single pile and pile group subjected to lateral spreading, the results showed that the bending moment developed in the pile was mainly caused by the lateral movement of the soft clay layer.

Previous studies on the behavior of the single pile or pile group located behind waterfront structures were often conducted in a qualitative manner; whereas, the quantitative study on the liquefied soil pressure on the pile caused by the lateral soil movement was limited. Dobry et al. [15] conducted six centrifuge model tests on the single pile foundations and calibrated two limit equilibrium methods, it was suggested that the liquefied soil pressure on pile was about 10.3 kPa. Japan Road Association (JRA) [16] and Japan Sewage Works Association (JSWA) [17] guidelines suggested a triangular pattern for the liquefied

* Corresponding author.

E-mail addresses: hit_tl@163.com (L. Tang), xianzhang_ling@263.net (X. Ling).

soil pressure, and lateral load on pile was expressed as a function of the sand density, pile length and pile diameter. With the shake-table test results, He et al. [18] advocated that the liquefied soil pressure on the pile approximately equaled to the total overburden stress. Haigh et al. [19] and Haigh and Madabhushi [20] suggested a uniform liquefied soil pressure of 16 kPa on the pile in liquefiable layer. Similarly, Gonzalez et al. [21] recommended a uniform pressure of 10 kPa. Tang et al. [22] suggested a uniform pressure of 19.5 kPa based on the measured data of a single pile shake-table test.

Although liquefied soil pressure induced by lateral spreading were suggested based on tests, the soil pressures suggested by different scholars could be significantly inconsistent [15,18–22]; thus, it is challenging to determine which pressure should be adopted in the practical design of pile foundations [23–28]. In addition, most of the existing lateral soil pressure were developed based upon the test results of the single pile, which are not able to be applied to the scenario in which the pile group is adopted [18–21]. In such a circumstance, JRA [16] and JSWA [17] proposed the liquefied soil pressure on the pile groups, in which the pressures on the individual pile in the pile group were assumed to be the same. The outcome of this assumption is that the bending moments of the individual pile in the pile group would be the same, however, this inference could not agree with the test results of the pile group [12,13]. Thus, one of the most important aspect of this study is to discuss and overcome this limitation, and give recommendation of liquefied soil pressure on the individual pile in the pile group.

In the following sections, a shake-table test on a 2×2 pile group behind a quay wall subjected to the lateral spreading is conducted, and the results are presented and analyzed first. On this basis, a finite element (FE) analysis is conducted to evaluate the liquefied soil pressure on the individual pile in the pile group. The liquefied soil pressures suggested by JRA and JSWA are then compared to that obtained from the FE analysis and the test results. Next, a comparison between the liquefied soil pressure on the individual pile in the group and that on single pile obtained from the single-pile test [29] is conducted. Further, a parametric study is conducted to investigate the influence of the pile diameter and the pile rotational stiffness on the behavior of the pile group. Finally, the concluding remarks are drawn based upon the presented results.

2. Description of shake-table test

A shake-table test of a pile group behind a sheet-pile quay wall embedded in the saturated sand (Fig. 1) was performed in this study, and this test was conducted at the Institute of Engineering Mechanics, China Earthquake Administration. In this shake-table test, a rectangular laminar container was used with the dimension of 1.7 m in height, 2.2 m in width, and 3.5 m in length, and detailed information of this laminar container was described in Sun et al. [30].

The soil profile in the test consisted of a saturated 1.5-m thick sand stratum behind the quay wall (Fig. 2). The thickness of the saturated sand stratum in the front of the quay wall was 1.0 m. The water table was at the ground surface. The sand stratum was prepared using the water sedimentation method [31]. The sand material employed in the shake-table test was obtained from Harbin, China and its properties are listed in Table 1. The relative density (D_r) of the sand stratum was 45–50%, and the saturated density of this sand was approximately 1900 kg/m^3 .

Prior to the preparation of the sand stratum, a 2×2 pile group of steel pipe piles, the outer diameter of which was 0.088 m, was installed behind the quay wall. In an attempt to achieve a fixed-end condition, the pile was inserted into a socket which was firmly connected to the base of the laminar container using ethoxyline resin. Static lateral pushover tests were performed on the pile group before the preparation of the sand stratum to evaluate the actual degree of fixity at the top and bottom of the pile group. The obtained rotational stiffness at the top

and bottom of pile group is summarized in Table 2. The pile space in the pile group was 3 times of the pile diameter in both longitudinal and transverse directions. The Young's modulus (E) of the pile group was obtained from two tension tests, and the result is listed in Table 2.

The quay wall was placed in the laminar container before the preparation of the soil stratum, and was connected to the container base using a pin connection. The top of the quay wall was temporarily constrained before and during the preparation of the sand stratum. Before the shaking, the constraint on the top of the quay wall was removed, which would lead to the lateral spreading of the sand behind the quay wall. The material property of the quay wall is listed in Table 3.

Various sensors were installed to record the different response of the soil-pile system throughout the shaking (Fig. 2). For example, raster displacement meter was used to record the displacement of the liquefied soil. The base excitation was a sinusoidal wave with a frequency of 2 Hz, and the amplitude of which was approximately 0.18 g (bottom plot of Fig. 3). During the first 2 s, the base excitation was gradually increased from 0 to 0.18 g. Note that the base excitation was applied in the direction of perpendicular to the quay wall.

3. Test results

To facilitate the analysis of the test results, the time history results were divided into three stages: Stage 1 (i.e., 0–2.5 s): prior to liquefaction; Stage 2 (i.e., 2.5–5.6 s): development of the liquefaction-induced lateral spreading; and Stage 3 (i.e., 5.6–15 s): convergence of the lateral spreading. In this study, the soil and pile displacements towards the waterside are defined as positive.

3.1. Excess pore pressure and acceleration

Figs. 3 and 4 show the free-field (see Fig. 2) acceleration and excess pore pressure (u_e) time histories, respectively. In Stage 1, the amplitude of the free-field acceleration increased rapidly and attained the peak acceleration. The recorded u_e built up rapidly and much of the stratum reached the initial liquefaction (i.e., u_e is equal to the initial effective vertical stress) during first few cycles of shaking. In Stages 2 and 3, the amplitude of free-field acceleration decreased gradually as the soil liquefaction then maintained constant at a low amplitude until the shaking ended, indicating that the liquefied sand lost most of the shear strength. The liquefaction level u_e maintained constant until the shaking ended. It was noted that the u_e time history at the 1.4 m depth only reached about 90% of initial vertical effective stress. In addition, only slight fluctuations were observed in the acceleration and u_e time histories, showing an absence of significant dilation in the free-field liquefied soil response [32].

Due to the soil liquefaction, the period of the ground surface is longer than that of base excitation, which showed a longer period response. The recorded u_e was slightly greater than the initial effective vertical stress at depth of 0.2 m, which may be caused by the sinking of pore pressure sensors [22,29].

Fig. 5 shows the acceleration time histories at the pile cap, ground surface, and the base. In Stage 1, the acceleration of the pile cap increased gradually as the base excitation increased, and the maximum acceleration amplitude of the pile cap was reached at the end of this stage. The maximum acceleration of the pile cap was approximately 0.3g, which was much larger than the amplitude of base excitation, and this showed an amplification effect of the soil-pile system. In Stage 2, the pile cap acceleration decreased gradually while the amplitude of base excitation maintained constant. In Stage 3, lower ground surface acceleration was observed, because of the liquefaction of the saturated sand and the loss of the shear strength. As a result, the pile group vibrated as the piles were mounted at the base and under the free vibration, thus, the acceleration amplitude of pile cap increased gradually and then maintained a constant of about 0.25g.



Fig. 1. Shake-table test on pile group.

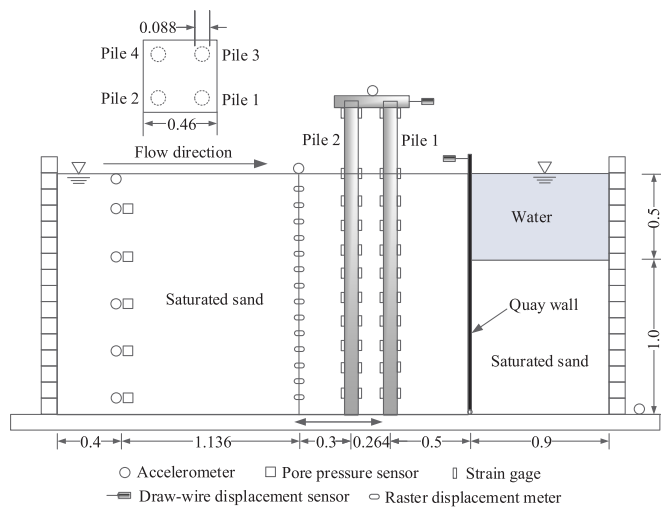


Fig. 2. Test setup and instrumentation (unit: m).

Table 1
Harbin Sand material properties.

Specific gravity	2.5
Maximum void ratio, e_{max}	0.89
Minimum void ratio, e_{min}	0.37
Coefficient of curvature, C_c	0.91
Coefficient of uniformity, C_u	2.98
Mean particle diameter, D_{50} (mm)	0.51
Fines content, F_c (%)	2

3.2. Displacement

In Stage 1, the lateral soil displacements (Fig. 6) oscillated cyclically and there was no significant deformation towards the quay wall. In Stage 2, the lateral soil displacements increased gradually due to the deformation of the quay wall. The lateral soil displacements increased on a cycle-by-cycle basis. In Stage 3, the amplitudes of the lateral soil displacements remained constant, and the quay wall reached the maximum displacement. The lateral soil displacement at the ground

Table 2
Pile group geometric and material properties.

Pile length (m)	1.95
Outside diameter (m)	0.088
Pile spacing (m)	0.264
Buried pile length (m)	1.5
Wall thickness (m)	6×10^{-4}
Moment of inertia (m^4)	1.57×10^{-7}
Young's modulus (GPa)	188
Rotational stiffness at pile bottom (N-m/rad)	25,500
Rotational stiffness at pile top (N-m/rad)	2100

Table 3
Steel quay wall geometric and material properties.

Height (m)	1.6
Width (m)	2.19
Thickness (m)	0.02
Young's modulus (GPa)	160

surface reached approximately 120 mm at the end of shaking. Lateral soil displacements near the ground surface were much larger than that near the base.

In Stage 1, the pile head displacement (Fig. 7) was similar to the soil displacement at the ground surface. In Stage 2, the pile head displacement reached the peak and then decreased slightly while the ground continued to displace laterally, which indicates that the liquefied soil lost most of the shear strength and began to flow around the pile group. The maximum pile head displacement was about 60 mm, which occurred at the beginning of Stage 2. In Stage 3, the pile head displacement continued to decrease and then remained constant, whereas the lateral spreading of the soil stopped in this stage. The permanent pile head displacement was 31 mm, which was much less than that of soil at the ground surface.

3.3. Pile bending moment

In Stage 1, the bending moment of the pile group (Fig. 8) increased gradually as the amplitude of the base excitation increased. In Stage 2, the bending moments of Pile 1 (i.e., the pile near the quay wall, see Fig. 2) and that of Pile 2 (i.e., the pile far from the quay wall, see Fig. 2)

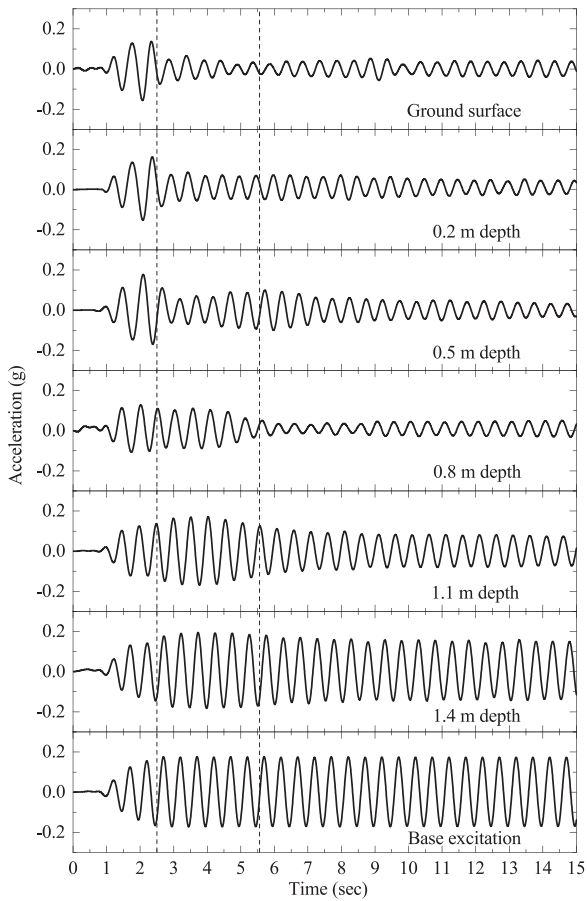


Fig. 3. Free-field acceleration time histories.

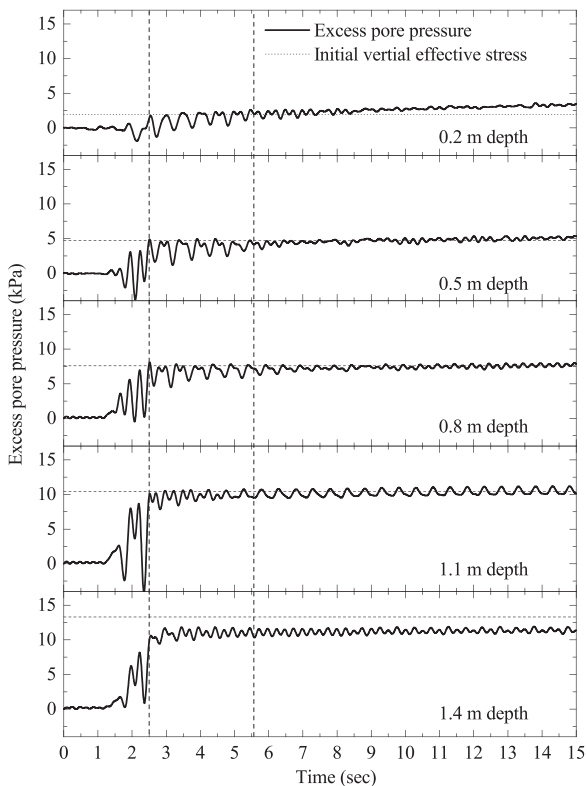


Fig. 4. Free-field excess pore pressure time histories.

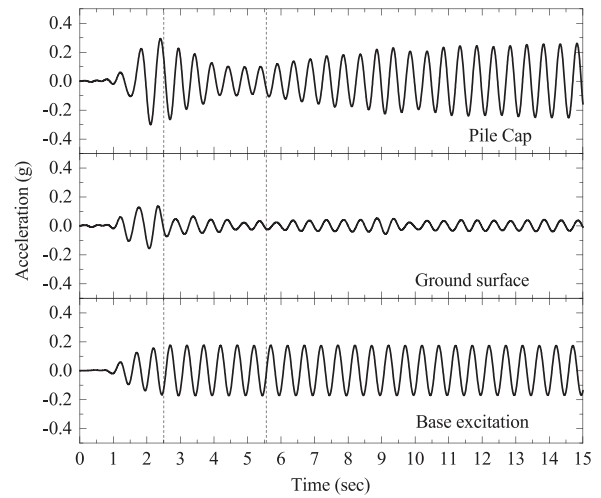


Fig. 5. Acceleration time histories at the pile cap, ground surface, and the base.

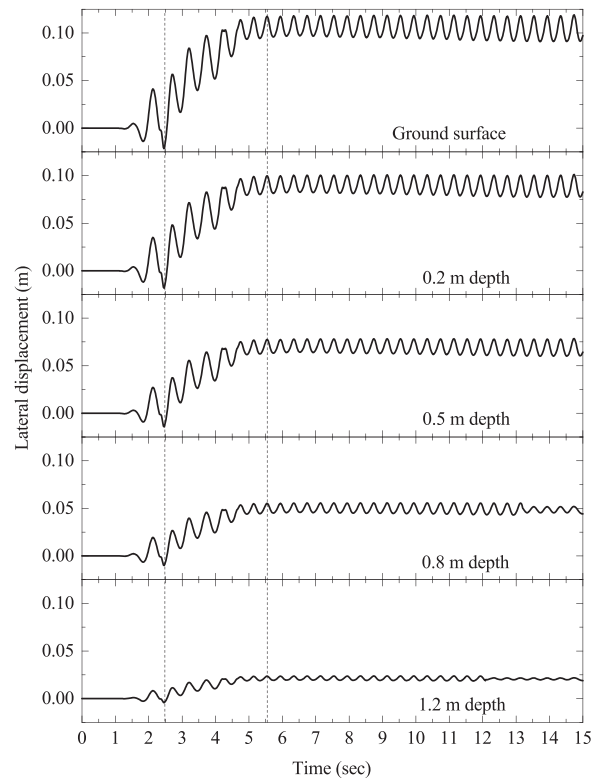


Fig. 6. Soil lateral displacement time histories.

rapidly reached the maximum values as the lateral soil displacement increased (Fig. 6). Then, the bending moments of the two piles began to decrease slightly, which was caused by the loss of soil strength and pile group partly bouncing back. In Stage 3, the bending moments of piles continued to decrease as the pile group bounced back, and then remained almost constant when the lateral soil displacement was stabilized.

The recorded bending moments (M_{rec}) could be decomposed into two components [11,22]: the monotonic part, M_{mon} , which is mainly caused by the soil lateral spreading (kinematic effect), and the cyclic part, M_{cyc} , which is caused by the soil and pile inertia effect. Here, FFT filter smoothing procedure with a cutoff frequency of 0.625 Hz was applied to the raw time histories of the bending moments, from which the monotonic bending moment M_{mon} could be obtained; and then, the cyclic bending moment M_{cyc} was calculated. For example, the time

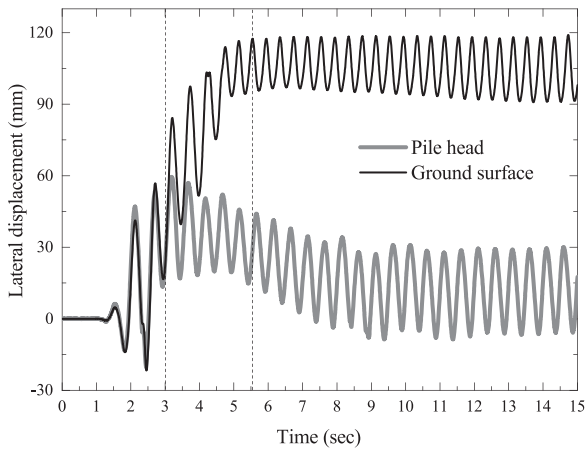


Fig. 7. Ground surface and pile head lateral displacement time histories.

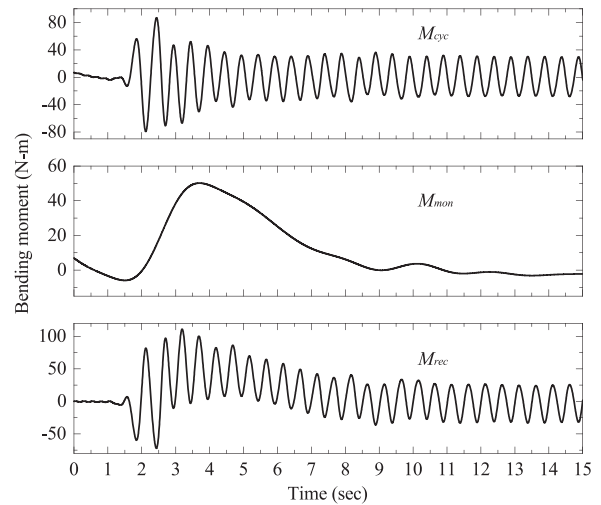


Fig. 9. Decomposition of Pile 1 bending moment time histories (at 1.1 m depth) into monotonic and cyclic components.

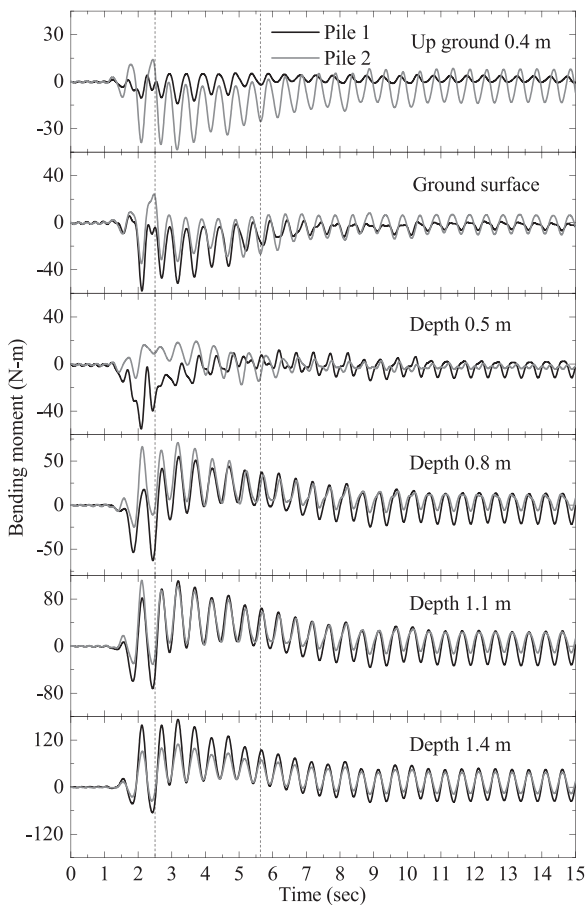


Fig. 8. Bending moment time histories at Piles 1 and 2.

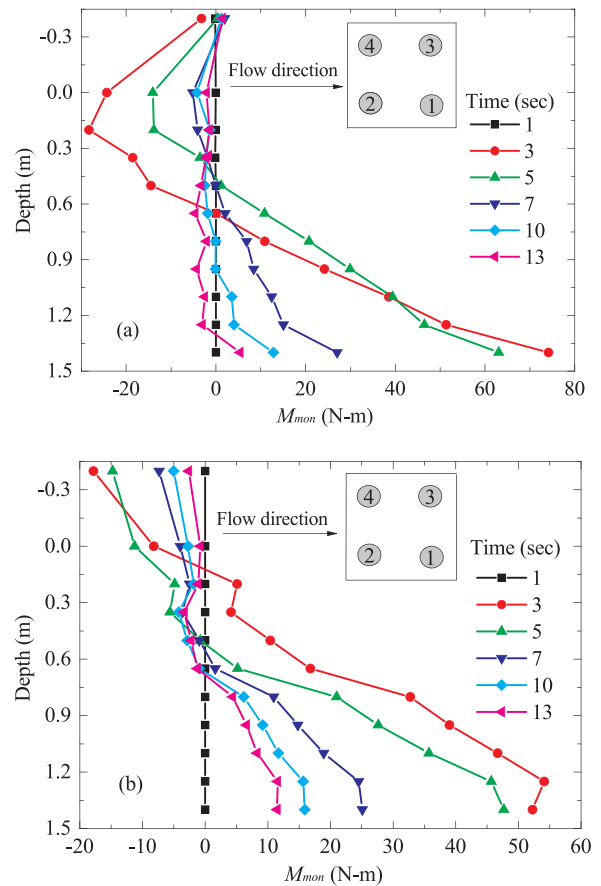


Fig. 10. Profiles of monotonic bending moment at different times: (a) Pile 1; (b) Pile 2.

history of the bending moment of Pile 1 at the depth of 1.1 m was decomposed into the cyclic and monotonic components, as shown in Fig. 9.

The profiles of M_{mon} of Piles 1 and 2 at different times are shown in Fig. 10. The maximum M_{mon} of Piles 1 and 2 at different time steps occurred at 1.4 m depth. As can be seen, the moment profiles of the pile group with a cap were distinctly different from that of a single pile showing the cantilever behavior [29]. Here, the bending moment response shown in Fig. 10 is qualitatively consistent with the results obtained in the past shake-table tests [8,13]. The profiles of maximum M_{mon} of Piles 1 and 2 are illustrated in Fig. 11. It is shown that these two piles within the group had similar bending moment response, more

specifically, the maximum bending moments of Piles 1 and 2 both occurred in the 1.4 m, and have similar trend along the depth, in addition, the bending moments on pile head of the two piles are both minus. It should be noted that the maximum bending moments of these two piles are quite different, i.e., Piles 1 and 2 sustained the largest positive M_{mon} of 83.3 N m and 58.4 N m at a depth of 1.4 m respectively. Due to the constraint of the pile cap, negative M_{mon} of -2.4 N m and -19.6 N m occurred at the pile head at Piles 1 and 2, respectively. Although the head displacements of Piles 1 and 2 were identical during the soil lateral flowing, the maximum bending moment (occurred in the bottom of

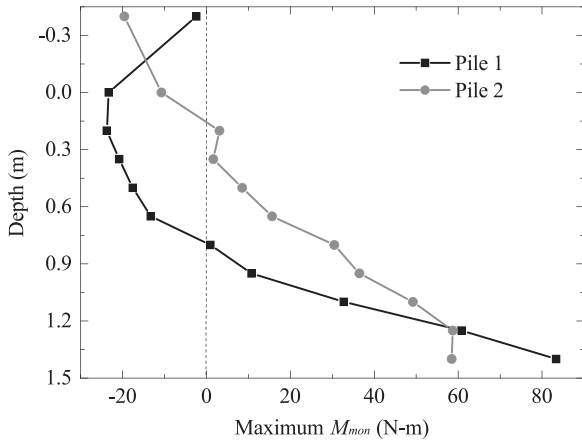


Fig. 11. Profiles of maximum monotonic bending moment at Piles 1 and 2.

the pile group) of Pile 1 was larger than that of Pile 2, which indicated the significance of the pile group effect. This phenomenon is termed as the shadowing effect [33]. The differences of M_{mon} between Piles 1 and 2 may be caused by the soil lateral spreading that started from the quay wall; as a consequence, Pile 1 was directly pushed by the laterally flowing soils, whereas Pile 2 was protected by Pile 1 against the direct impact of the lateral spreading, thus, the Pile 2 sustained less lateral load comparing to the Pile 1. Further, it could be noted that the behavior of the individual pile in the pile group behind the quay wall could be different from the behavior of the pile installed in mild slope obtained by Haeri et al. [26].

4. Modelling of the pile group response under lateral spreading

For a single pile, JRA [16] suggests that the triangular liquefied soil pressure on the pile could be computed as follows:

$$q_L = C_s \times C_L \times \gamma_L \times z \times D \tag{1}$$

where q_L in kN/m is the lateral soil pressure on a pile in the liquefiable layers at the depth z ; C_s is a modification factor that accounts for the influence of the distance from the water front, which is assumed to be 1 when the length of the pile is less than 50 m; C_L is a modification factor of the lateral pressure in a liquefiable layer, which is often taken as 0.3; γ_L is the averaged unit weight of the liquefiable layer (kN/m³); and, D is the pile diameter (m). For a pile group, JRA considers the pile group as an equivalent pile and assumes that the lateral soil pressure, determined as follows, is equally distributed among the piles:

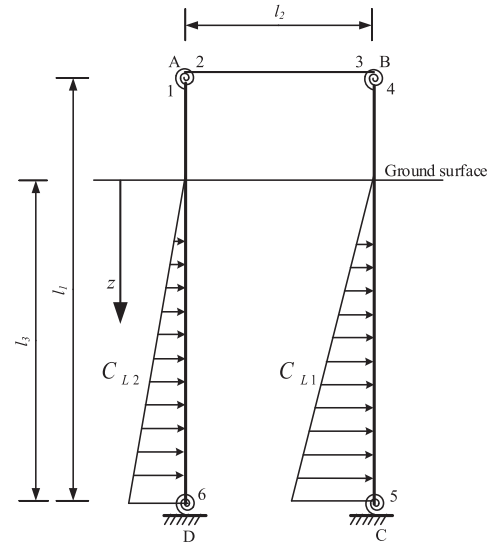
$$q_L = (C_s \times C_L \times \gamma_L \times z \times W) / n \tag{2}$$

where W is the width of pile group, and n is the total number of piles in the pile group.

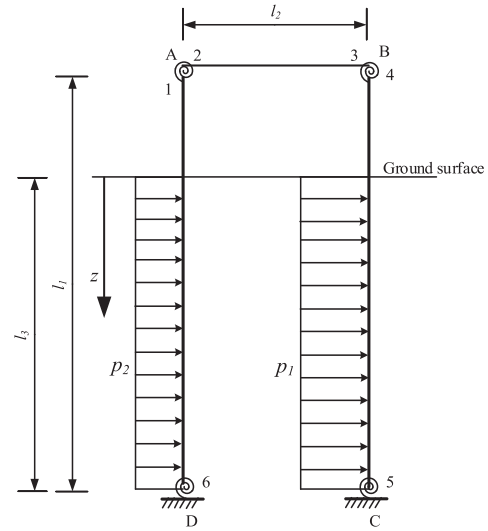
JSWA [17] also recommends the lateral soil pressure for the pile group analysis and design. JSWA assumes that the identical liquefied soil pressure acts on the individual pile in the pile group. JSWA suggests that the liquefied soil pressure acting on the individual pile in the pile group should be calculated using the pile diameter rather than the pile group width, and the triangular soil pressure on the pile is estimated as follows.

$$q_L = 0.05 \times D \times \gamma_L \times z \tag{3}$$

A FE model was developed herein (Fig. 12), in which, the piles were assumed to be linearly elastic under the lateral spreading, the pile group was modeled as a plane frame, and rotational springs were used to simulate the rotational stiffness at the top and bottom of the pile. In this study, the pile length l_1 was taken as 1.95 m, the pile spacing l_2 was taken as 0.264 m, and the thickness of soil layer l_3 was taken as 1.5 m. Static lateral loads that imitate the liquefied soil pressures were applied on the pile shafts and M_{mon} of the pile group was computed using this



(a) $C_{L1}=C_{L2}=0.3$, JRA (2002)
 $C_{L1}=C_{L2}=0.05$, JSWA (1997)
 $C_{L1}=0.19$, $C_{L2}=0.092$, this study



(b) $p_1=1.31$ kPa, $p_2=0.66$ kPa, this study

Fig. 12. Finite element model for analysis of piles subjected to liquefied soil pressures: (a) triangularly-distributed soil pressure; (b) uniformly-distributed soil pressure.

FE model.

Two liquefied soil pressure distribution scenarios, as shown in Fig. 12, were analyzed in this study. The p_1 and p_2 represent the uniform soil pressure on the piles near the quay wall and far from the quay wall, respectively; and, C_{L1} and C_{L2} are the modification factors of the triangular soil pressure (see Eqs. (1) and (2)) on the pile near the quay wall and far from the quay, respectively. After repeating trials, it was found that the M_{mon} computed using p_1 of 1.31 kPa and p_2 of 0.66 kPa or C_{L1} of 0.19 and C_{L2} of 0.092 could match the tested M_{mon} (Fig. 13), especially at shallow depths.

Fig. 13(a) shows the liquefied soil pressure on Pile 1, which indicates that the liquefied soil pressure proposed by JRA [16] is slightly higher than that of the present study, while, the liquefied soil pressure of JSWA guideline [17] is much smaller than that of the present study. Hence, the JSWA guideline underestimates the bending moment of Pile 1 (Fig. 13(b)), whereas the JRA guideline overestimates the bending moment of Pile 1. Fig. 13(c) depicts the liquefied soil pressure on Pile 2, which shows that the liquefied soil pressure given by JRA is much

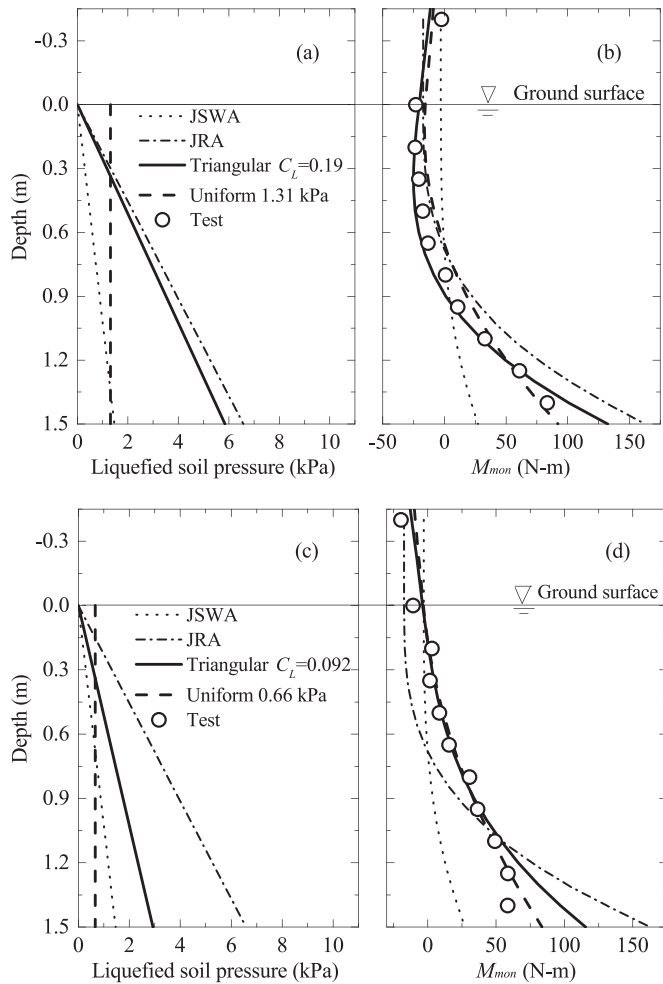


Fig. 13. Comparison of soil pressures and bending moments: (a) liquefied soil pressure on Pile 1; (b) M_{mon} of Pile 1; (c) liquefied soil pressure on Pile 2; (d) M_{mon} of Pile 2.

higher than that of the present study, while liquefied soil pressure suggested by JSWA is less than that suggested by this study. Similarly, the JRA guideline overestimates the M_{mon} of Pile 2, while the JSWA guideline underestimates the results (see Fig. 13(d)). By comparing the liquefied soil pressure on the individual pile in the group, it is found that the liquefied soil pressure on Pile 1 is about twice of that on Pile 2 for both uniform and triangular soil pressure patterns, which is contrast with the liquefied soil pressure suggested in JRA [16] and JSWA [17] for pile group.

5. Discussion

5.1. Comparison of liquefied soil pressures on single pile and 2×2 pile group

Su et al. [29] studied the pile response to the liquefaction-induced lateral spreading using a 1-g shake-table test, and adopted two liquefied soil pressure distributions (i.e., triangular and uniform) to evaluate the single pile behavior subjected to the lateral spreading. The facilities and test conditions involved in this single-pile test and the test conducted in this study were nearly identical.

Table 4 summarized the triangular and uniform soil pressures on the single pile suggested by Su et al. [29] and the pressure on the individual pile in the pile group developed by this study. The data in Table 4 shows that both triangular and uniform liquefied soil pressures on the pile group are much less than that on the single pile, which is caused by group effect.

Table 4
Liquefied soil pressures of single pile and pile group.

	Single pile [29]	Pile 1		Pile 2	
		Value	Ratio (R_1)	Value	Ratio (R_2)
C_L of triangular soil pressure	0.7	0.19	0.271	0.092	0.131
Uniform soil pressure (kPa)	4.8	1.31	0.273	0.66	0.138

The ratio of the liquefied soil pressure on Pile 1 (given by this study) over that on the single pile (suggested by Su et al. [29]) is defined as R_1 . Similarly, the ratio of the liquefied soil pressure on Pile 2 over that on the single pile is defined as R_2 . From Table 4, R_1 of both triangular and uniform liquefied soil pressures are about 0.27, and R_2 of both triangular and uniform liquefied soil pressures are about 0.13, which indicates R_1 and R_2 of the triangular and uniform liquefied soil pressures are quite consistent. This consistency of R_1 and R_2 shows the liquefied soil pressure developed in this study are reasonable. The difference of the liquefied soil pressures between the pile group and the single pile could be explained by the group effect.

5.2. Parametric study

In this section, a parametric study was conducted to investigate the effects of the pile rotational stiffness and the pile diameter on the distributions of the bending moment along the pile group using the FE model and the suggested liquefied soil pressure (mentioned in Section 4).

5.2.1. Influence of rotational stiffness at bottom of piles, K_b

The influence of the rotational stiffness at pile bottom on the bending moments of pile group is shown in Fig. 14. The pile diameter and rotational stiffness at the top of the pile remain the same as the measured values. In this parametric study, the value of K_b varied in the range of $0.1\text{--}1.0 \times 10^{11}$ N-m/rad, which represents the pin to fixed boundaries, respectively. The circles (Fig. 14) represents the calculated bending moments using the measured rotational stiffness. It is seen that the rotational stiffness affects pile bending moments significantly, and the influence becomes less significant with the increase of K_b . Herein, the bending moments at pile bottom increase with the rotational stiffness; the bending moments at the top of piles decrease with increasing K_b , and, the influence becomes insignificant after K_b reaches 12,750 N-m/rad. The maximum bending moment occurred at the bottom of pile group when the rotational stiffness at the bottom is quite large, which explains that piles were damaged at the bottom during the earthquake if the piles are located within a stiff stratum.

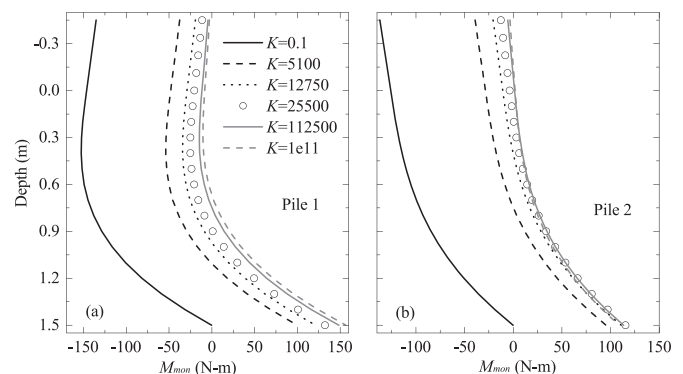


Fig. 14. Influence of rotational stiffness at bottom of pile group on bending moment.

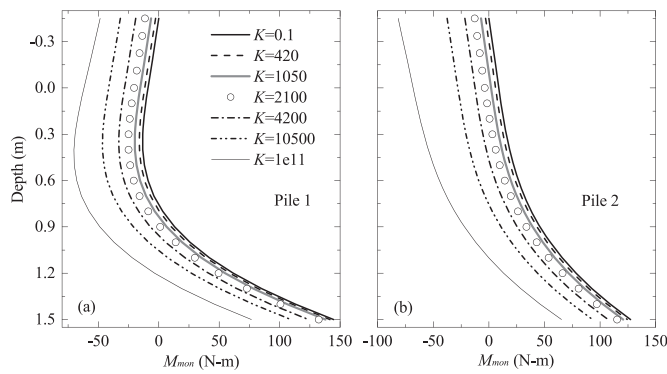


Fig. 15. Influence of rotational stiffness at top of pile group on bending moment.

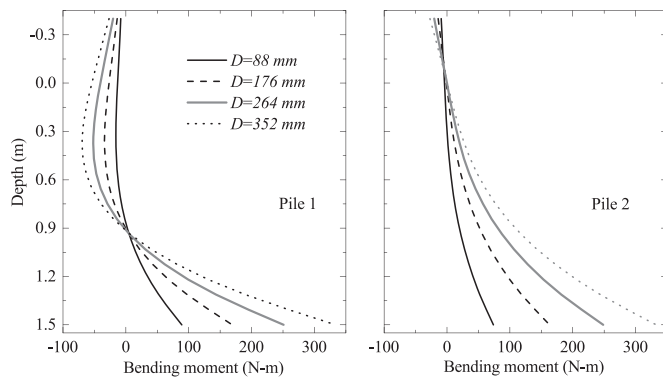


Fig. 16. Influence of pile diameter on bending moment.

5.2.2. Influence of rotational stiffness at top of piles, K_t

Fig. 15 shows the influence of the rotational stiffness at the pile top on the bending moments of the pile group. The K_t of 0.1 N-m/rad represents a pin connection and 1.0×10^{11} N-m/rad represents a fixed connection at the top of piles. A variation of K_t from 0.1 to 1.0×10^{11} N-m/rad caused an obvious increase in the pile head bending moments and decrease in pile base bending moments for both Piles 1 and 2. This result indicates that K_t affects the pile group bending moments significantly. The maximum bending moments of piles occurred on pile head under the situation of $K = 1.0 \times 10^{11}$ N-m/rad, which implies that larger bending moments could be generated at the pile head, and the pile can be damaged on the top in the liquefaction-induced lateral spreading ground if the degree of fixity on pile head is quite large.

5.2.3. Influence of pile diameter, D

Based on the FE model and Eqs. (1) and (2), the soil pressure would be a function of the pile diameter. Fig. 16 shows the effect of the pile diameter on the bending moments of the pile group, in which the pile diameter ranges from 44 mm to 352 mm while the other parameters are the same with that of shake-table test. It is found that the bending moments of the piles in the group increases with the pile diameter, especially at the greater depth. During the lateral spreading of the saturated sand, a larger pile diameter could mobilize a greater soil wedge behind the pile and result in a larger soil pressure. As a result, the bending moment of the individual pile in the pile group would dramatically increase with the pile diameter.

6. Conclusions

This study mainly investigates the response of a 2×2 pile group and the lateral soil pressures acting on individual piles in the pile group subjected to liquefaction-induced lateral spreading. The main conclusions are summarized as:

- (1) The free field acceleration amplitude decreases significantly as sand stratum liquefied fully and the excess pore pressure maintains constant until the end of shaking. Permanent pile head displacement is approximately 31 mm that is far less than the ground surface displacement of 120 mm. The monotonic bending moment of the pile near the quay wall is larger than that of the pile far from the quay wall, which shows an obvious shadowing effect of the pile group.
- (2) The plane frame finite element model with rotational springs can reproduce the bending moment response of the 2×2 pile group subjected to lateral spreading. The uniform soil pressure, p_1 of 1.31 kPa on the pile near the quay wall and p_2 of 0.66 kPa on the pile far from the quay wall, are found to be able to approximate the tested bending moments. The modification factors of triangular soil pressure, C_{L1} of 0.19 on the pile near the quay wall and C_{L2} of 0.092 on the pile far from the quay wall, are also acceptable to match the observed bending moments.
- (3) For both uniform and triangular soil pressure scenarios, the liquefied soil pressure on the pile near the quay wall is about twice as much as that on the pile far from the quay wall. The JRA guideline may overestimate the bending moments of the 2×2 pile group, however, the JSWA guideline seems to underestimate the results. Both triangular and uniform liquefied soil pressures on individual pile in the pile group are far less than those on single pile.
- (4) The pile rotational stiffness and diameter can significantly affect the pile group response. The pile base has a better chance to be damaged during earthquake if the pile is located within a quite stiff stratum; larger bending moments could be generated at the pile head and pile may be damaged at pile head if the pile head-cap connection is stiffer; pile group bending moment is able to increase dramatically as the diameter increases.
- (5) Additional experimental data included shake table, centrifuge and field tests should be conducted to further explore the liquefied soil pressure and complex patterns of soil-pile interaction under lateral spreading.

Acknowledgments

This work was supported by the National Natural Science Foundation of China (Grant Nos. 51578195, 51378161 and 51308547), and the Open Research Fund of State Key Laboratory of Geomechanics and Geotechnical Engineering, Institute of Rock and Soil Mechanics, Chinese Academy of Sciences, under Grant No: Z016007. Prof. L. Jing, Prof. X. Yuan, and Dr. Y. Wang at the Institute of Engineering Mechanics, China, assisted in the shake-table experiment. The first author is grateful to Harbin Institute of Technology for funding the academic visit to the University of Alberta.

References

- [1] Hamada M. Large ground deformations and their effects on lifelines: 1964 Niigata earthquake [Technical report NCEER-92-0001]. New York: US National Center for Earthquake Engineering Research; 1992. p. 1–123.
- [2] Boulanger RW, Mejia LH, Idriss IM. Liquefaction at Moss Landing during Loma Prieta earthquake. *J. Geotech. Geoenviron. Eng.* 1997;123:453–67.
- [3] Sugimura Y, Karkee MB, Mitsuji K. An investigation on aspects of damage to precast concrete piles due to the 1995 Hyogoken-Nambu Earthquake. In: Proceedings of the 3rd UJNR workshop on soil-structure interaction. California; 2004. p. 1–16.
- [4] Hamada M, Daigaku T, Gakubu K. Study on liquefaction induced permanent ground displacements. Japan: Association for the Development of Earthquake Prediction; 1986.
- [5] Gómez J, Tavera H, Orihuela N. Soil liquefaction during the Arequipa Mw 8.4, June 23, 2001 earthquake, southern coastal Peru. *Eng Geol* 2005;78:237–55.
- [6] Haskell J, Madabhushi S, Cubrinovski M, Winkley A. Lateral spreading-induced abutment rotation in the 2011 Christchurch earthquake: observations and analysis. *Geotechnique* 2013;63(15):1310–27.
- [7] Tang L, Ling XZ. Response of a RC pile group in liquefiable soil: a shake-table investigation. *Soil Dyn Earthq Eng* 2014;67(12):301–15.
- [8] Tang L, Zhang XY, Ling XZ, Su L, Liu CH. Response of a pile group behind quay wall to liquefaction-induced lateral spreading: a shake-table investigation. *Earthq Eng*

- Eng Vib 2014;13(4):741–9.
- [9] Sato M. Reproduction of seismic liquefaction damage to caisson type quay wall and its neighboring pile foundation in a centrifuge model. *J Geotech Eng Jpn Soc Civil Eng* 1997;295–304. [in Japanese].
- [10] Sato M, Tabata K. Lateral spreading damage to sheet-pile walls and pile foundations reproduced by Tsukuba large-scale shake table. *J Earthq Tsunami* 2011;5(03):231–40.
- [11] Motamed R, Towhata I. Shaking table model tests on pile groups behind quay walls subjected to lateral spreading. *J Geotech Geoenviron Eng* 2010;136:477–89.
- [12] Motamed R, Towhata I, Honda T, Tabata K, Abe A. Pile group response to liquefaction-induced lateral spreading: E-defense large shake table test. *Soil Dyn Earthq Eng* 2013;51:35–46.
- [13] Motamed R, Towhata I, Honda T, Yasuda S, Tabata K, Nakazawa H. Behaviour of pile group behind a sheet pile quay wall subjected to liquefaction-induced large ground deformation observed in shaking test in E-defense project. *Soils Found* 2009;49:459–75.
- [14] Ashford SA, Juirnarongrit T, Sugano T, Hamada M. Soil-pile response to blast-induced lateral spreading. I: field test. *J Geotech Geoenviron Eng* 2006;132:152–62.
- [15] Dobry R, Abdoun T, O'Rourke T, Goh S. Single piles in lateral spreads: field bending moment evaluation. *J Geotech Geoenviron* 2003;129:879–89.
- [16] Japan Road Association. Design specification of highway bridges-Part V: seismic design. Tokyo, Japan; 2002.
- [17] Japan Sewage Works Association. Seismic counter measure guidelines for sewage facilities; 1997. p. 90–1. [in Japanese].
- [18] He L, Elgamal A, Abdoun T, Abe A, Dobry R, Hamada M, et al. Liquefaction-induced lateral load on pile in a medium D_v sand layer. *J Earthq Eng* 2009;13:916–38.
- [19] Haigh S. Effects of earthquake-induced liquefaction on pile foundations in sloping ground [Ph.D. thesis]. Cambridge: University of Cambridge; 2002.
- [20] Haigh S, Madabhushi S. Centrifuge modelling of lateral spreading past pile foundations. In: Proceedings of the 2nd international conference of physical modelling in geotechnics. Newfoundland, Canada; 2002. p. 471–5.
- [21] González L, Abdoun T, Dobry R. Effect of soil permeability on centrifuge modeling of pile response to lateral spreading. *J Geotech Geoenviron Eng* 2009;135:62–73.
- [22] Tang L, Ling XZ, Zhang XY, Su L, Liu CH, Li H. Response of a RC pile behind quay wall to liquefaction-induced lateral spreading: a shake-table investigation. *Soil Dyn Earthq Eng* 2015;76:69–79.
- [23] Su L, Tang L, Ling XZ, Ju NP, Gao X. Responses of reinforced concrete pile group in two-layered liquefied soils: shake-table investigations. *J Zhejiang Univ Sci A* 2015;16(2):93–104.
- [24] Abdoun T, Dobry R, O'Rourke TD, Goh SH. Pile response to lateral spreads: centrifuge modeling. *J Geotech Geoenviron Eng* 2003;129(10):869–78.
- [25] Brandenburg SJ, Boulanger RW, Kutter BL, Chang D. Behavior of pile foundations in laterally spreading ground during centrifuge tests. *J Geotech Geoenviron Eng* 2005;131:1378–91.
- [26] Haeri SM, Kavand A, Rahmani I, Torabi H. Response of a group of piles to liquefaction-induced lateral spreading by large scale shake table testing. *Soil Dyn Earthq Eng* 2012;38:25–45.
- [27] Imamura S, Hagiwara T, Tsukamoto Y, Ishihara K. Response of pile groups against seismically induced lateral flow in centrifuge model tests. *Soils Found* 2004;44:39–55.
- [28] Rollins KM, Gerber TM, Lane JD, Ashford SA. Lateral resistance of a full-scale pile group in liquefied sand. *J Geotech Geoenviron Eng* 2005;131:115–25.
- [29] Su L, Tang L, Ling XZ, Liu CH, Zhang XY. Pile response to liquefaction-induced lateral spreading: a shake-table investigation. *Soil Dyn Earthq Eng* 2016;82:196–204.
- [30] Sun H, Jing L, Meng X, Wang N. A three-dimensional laminar shear soil container for shaking table test. *J Vib Shock* 2012;31:26–32. [in Chinese].
- [31] Ishihara K. Liquefaction and flow failure during earthquakes. *Geotechnique* 1993;43(3):351–415.
- [32] Zeghal M, Elgamal A, Parra E. Identification and modeling of earthquake ground response-II. Site liquefaction. *Soil Dyn Earthq Eng* 1996;15(8):523–47.
- [33] Rollins KM, Peterson KT, Weaver TJ. Lateral load behavior of full-scale pile group in clay. *J Geotech Geoenviron Eng* 1998;124:468–78.